

A Portable Device for Screw Theory Characterization of the Human Ankle

Un dispositivo Portátil para la Caracterización de la Teoría de Tornillos del Tobillo Humano

Julio H. Vargas R¹, Angel Valera², Óscar Agudelo Varela³

^{1,2} Universitat Politècnica de Valencia Instituto de Automática e Informática Industrial Ai2 Valencia, Spain

³ Universidad de los Llanos Facultad de Ciencias Básicas e Ingeniería Villavicencio, Meta, Colombia

¹julio_h_vargas_r@ieeee.org, ²giuprog@isa.upv.es, ³oscar.agudelo@unillanos.edu

Abstract—This article present a device for spatial pose localization of the human foot respect to the leg. Uses the concept of irregular tetrahedron geometry for the apex from the plane base vertices localization. The pose is given in screw theory notation, relative to a reference frame on the shank. The device is based on simple wire sensors as alternative to optical systems. The device was designed for cheap, easy construction, use and assembly for general users as the bio-mechanics community. A model approximation is used and complemented with two Motion Processing Units for sensor fusion.

Keywords—Ankle, robot, Motion capture. Kinematics. Tetrahedron solving

I. INTRODUCTION

Human joints haven't exact equivalent mechanical joints, like prismatic or hinge joints. Therefore, the measurement of position and orientation is difficult to accomplish. For the human ankle, the basic instruments are the metric tape and the *goniometer*. Mocap devices are used in prepared ambiances, generally designed for the whole human body. Is needed attach markers or sensors, and use many calibrated cameras. In outdoors, dirty environments, with fog, fumes, vapor or dust, dust ambiances, the vision systems would fail due to light reflection or camera obstruction. The cost of such systems is expensive and aren't portable and specific for the ankle. The patients need translated to a such ambiances with cameras disposed and the angles of the joints are estimated by post-processing and filtering the optical data captured.

The ankle is composed of several joints of various bones. The main bones are the tibia, the fibula, the talus and calcaneus. In this work, we present a device for capture the ankle data in a screw theory characteristic function, named exponential transformation.

II. PREVIOUS WORK

Searching in literature, the position and orientation of the ankle has two approaches, *in vivo* (living people, non invasive) and *in vitro* (cadaver, invasive). Generally is based on bi-axial models, taloclural and tibiotalar axis. One of the first measurements were taken *in vitro* [1]. In this work the pose is taken on terms of infinitesimal screw theory[2]. The axis of rotation of the ankle is researched in [3] by using a mechanical platform. In [4] *in vitro* ankle kinematics was studied by means of photography and a mechanical method with pins attached

to mobile parts. In [5] the bones contact surface was analyzed, as the external and internal forces acting on the joint. In [6] a method is used for application in aligning articulated boots. In [7], an ingenious ankle locator is presented, by using radiography and applying load to the foot. In [8] an *in vitro* method is applied, using markers on the tibia, talus and calcaneus.

In vivo measurements were taken on specific patients in [9], MRI technology and markers processing was used. The work of [10], presents a specific ankle estimation by using optical markers, optimization, and, comparing free and loaded movements. The work in [11] present a three dimensional reconstruction of the bones for the axis estimation. In [12] optical markers were used for validation of the palpation method of localization. In [13] dual-fluoroscopy was used for get models of one and three degrees of freedom, and validated with optical markers. In [14] MRI was used for ankle estimation of patient specific with juvenile idiopathic arthritis. The book [15] presents a complete computational model of the ankle kinematics.

Screw theory representation is used in [16], applying the concept of infinitesimal screw triangle as in texts like [17] and [18].

III. METHODOLOGY

Our proposed solution was designed taking into account characteristics as: easy of use, accessible and cheap components and open source approach. The basic element is a 3D printed draw wire sensor built from a retractile element and a multi-turn potentiometer.

The geometrical analysis is made by using tetrahedron geometry, the localization of the apex is computed from the distance to the vertices of the base triangle. In the figure 1 the method is illustrated.

In the figure 1, the base triangle is defined by the triangle with vertices $A = (A_x, A_y, A_z)$, $B = (B_x, B_y, B_z)$, $C = (C_x, C_y, C_z)$, and the origin O is located at the same plane. For each vertex, an equilateral triangle is defined, $A_1 =$

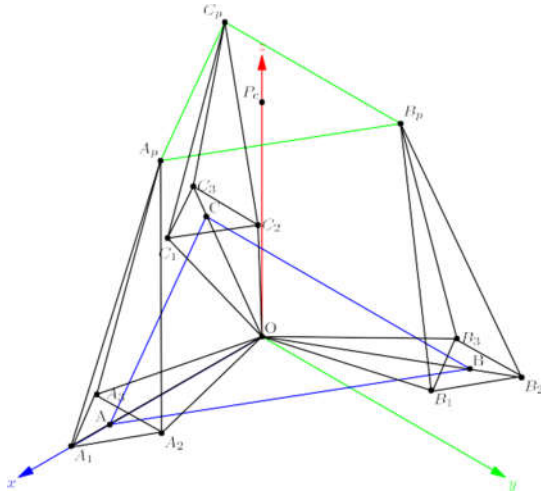


Fig. 1. Schematic of the localization method

$(A_{1x}, A_{1y}, A_{1z}), A_2, A_3, B_1, B_2, B_3,$ and, $C_1, C_2, C_3.$ The mobile platform is defined by the triangle vertices $A_p, B_p, C_p,$ and the platform reference system is located in the point $P_c.$

Defining the irregular tetrahedron with the vertices $T_A = \{A_1, A_2, A_3, A_p\}.$ The length of the sides from the triangle of the base A_1, A_2, A_3 to the apex A_p can be defined as:

$$l_{1A} = \|A_p - A_1\|$$

$$l_{2A} = \|A_p - A_2\|$$

$$l_{3A} = \|A_p - A_3\|$$

the triangle base vertices A_1, A_2, A_3 and the distances l_{1A}, l_{2A}, l_{3A} are known, and the apex $A_p = (A_{px}, A_{py}, A_{pz})$ can be solved geometrically, by using spheres intersection. The coordinates of A_p are:

$$A_{px} = \frac{l_{2A}^2 + l_{3A}^2 - 2l_{1A}^2}{6r} \quad (1)$$

$$A_{py} = \frac{\sqrt{3}l_{3A}^2 - \sqrt{3}l_{2A}^2}{6r} \quad (2)$$

$$A_{pz} = \frac{\sqrt{-9r^4 + 3\lambda_1 r^2 - \lambda_2} + \lambda_3}{3r} \quad (3)$$

where r is the radius from the center point A to the vertices of the equilateral triangle $A_1A_2A_3,$ and, for the sake of reduce notation: $\lambda_1 = l_{1A}^2 + l_{2A}^2 + l_{3A}^2, \lambda_2 = l_{1A}^4 + l_{2A}^4 + l_{3A}^4, \lambda_3 = l_{1A}^2 l_{2A}^2 + l_{1A}^2 l_{3A}^2 + l_{2A}^2 l_{3A}^2.$ Is important to notate that there are recursive calculations in the equations, useful for real-time measurements.

The number of sensors depends on the lengths $l_{1A}, l_{2A}, l_{3A},$ which are edges of the tetrahedron $T_A,$ which are three. For each one for the remaining tetrahedrons are needed three sensors. A total of nine sensors should be needed.

The number of sensors can be reduced from nine to seven, or six, if we know the platform's dimensions. First, solving

the apex A_p of the tetrahedron $T_A.$ The position of the two remaining apex B_p, C_p can be solved with sphere intersection method, taking the apex A_p as the center of spheres with radius $r_{ba} = \|B_p - A_p\|$ and $r_{ca} = \|C_p - A_p\|.$

The condition of sensor reduction is at expenses of the speed of computation. The computes must be sequential, first the apex A_p and then the other two B_p and $C_p.$ This can be useful in multi-thread, multi-core or FPGA based systems.

A. Sensor design

The main element of the device is the draw wire sensor, this sensor is composed from a multi-turn potentiometer, a flat spring retractile element, a pulley and a wire for measurement.

The figure 2 shows the element sensor, is a retractile element with a commonly used multi-turn potentiometer.

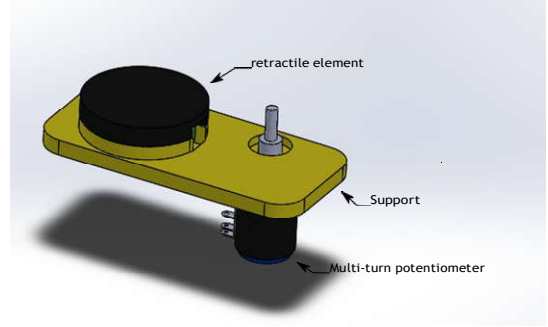


Fig. 2. Draw Wire Sensor

The pulley is designed for avoid slippery of the wire, works like a double winch. Line fishing is used and attached to the pulley, is a two coil system, when one is rolled the other is extended. the figure shows the pulley double coil design.

An array of sensors is showed in the figure

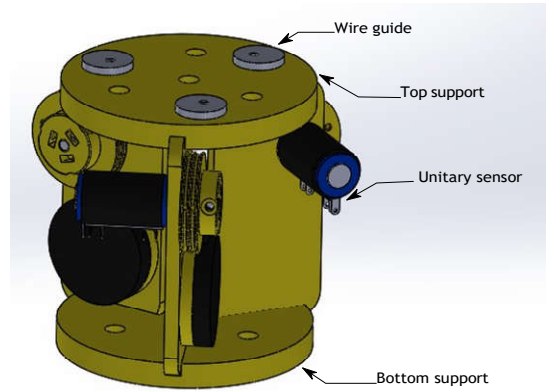


Fig. 3. Array of sensors

Each potentiometer is connected to a electronic shield.

B. Signal conditioning circuit

The electronics for the device is the two instrumentation operational amplifier circuit. We have designed a capture

shield for all the sensors. Each sensor is calibrated with the level and amplification maximum for full range ADC capture of the Arduino board.

The objective is to maintain a low cost sensor, and easy for maintenance. We select a ten turns potentiometer, with a flat spring with maximal compression of four turns. With $R_{nom} = 2.2k\Omega$, ten turns, gives $R_{turn} = 220\Omega$ per turn. Starting from a resistance of $R_{ini} = 200\Omega$, the resistance after four turns R_{max} is:

$$R_{max} = R_{ini} + 4R_{turn} = (200 + 880) \Omega = 1080\Omega$$

The diameter of the pulley is $D = 38mm$, the spring can be compressed four turns, the maximal measurement of the sensor is:

$$d_{max} = 4 \cdot D \cdot \pi \approx 477.5mm$$

The input is a Wheatstone bridge, the values of the resistors are balanced from zero difference to a maximum value. The voltage divider is given by a $R_1 = 100k\Omega$ resistor and $R_2 = 200\Omega$ voltage divider. The value of the reference source is $V_r = 5V$, the voltage divider V_{d1} is:

$$V_{d1} = \frac{V \cdot R}{R_1 + R_2}$$

$$(5 \cdot 200)/(10^5 + 200) = 0.0099800 \approx 10mV$$

The voltage V_{d2} computed from the maximal resistance $R_{max} = 880\Omega$ is:

$$V_{d2} = \frac{V_r \cdot R_{max}}{R_1 + R_{max}}$$

$$(5 \cdot 880)/(10^5 + 880) = 0.043616 \approx 44mV$$

The input voltage for the amplifier is:

$$V_i = V_{d2} - V_{d1} = 34mV$$

For the two Op. Amp. instrumentation amplifier the output V_o is:

$$\frac{V_o}{V_i} = 1 + \frac{R_2}{R_1} + \frac{2R_2}{R_G}$$

Selecting $R_2 = 100k\Omega$ and $R_1 = 1k\Omega$, and $R_G = 5k\Omega$, the gain $\frac{V_o}{V_i}$ is:

$$1 + \frac{10^5}{10^3} + \frac{2 \cdot 10^5}{5 \cdot 10^3} = 141$$

for 34mV, we obtain:

$$141 \cdot 0.034 = 4.794V$$

The basic circuit is showed in the figure

For the software acquisition, an exponential moving average (EMA) filter is used for avoid noise problems in the potentiometer. The main algorithm is:

$$S_t = a \cdot Y_t + (1 - a) \cdot S_{t-1}$$

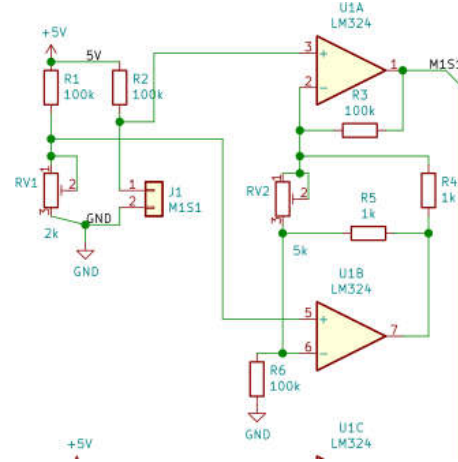


Fig. 4. Two Op. Amp. instrumentation amplifier

Where S_t is the output of the filter on actual time t , a is a weight factor of the actual reading Y_t , and S_{t-1} is the filter output in anterior time $t-1$.

Adding connection for the two MPUs and the OLED and two potentiometers for measuring the battery packs, and buck and boost circuits for 12V and 5V from two 18650 batteries with Battery management systems. And designing for seven sensors and using throw hole for easy assembly and measurements, the shield is showed in the figure.

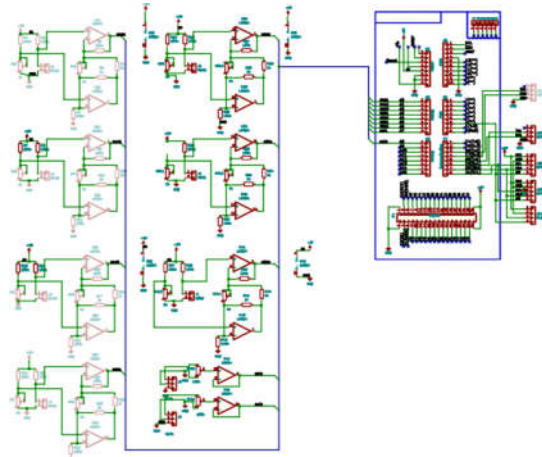


Fig. 5. Complete schematic

The final appearance of the shield is showed in the figure. This figure was exported to 3D CAD and the dimensions of all the components were used for the box design.

C. Distribution of the mechanical components and final assembly

The box design is compact and portable, there are fan system, battery system and BMS, for the Arduino and Orange PI. All the components are located in the box. The electronics box is attached to a aluminum structure. A 3D printed leg

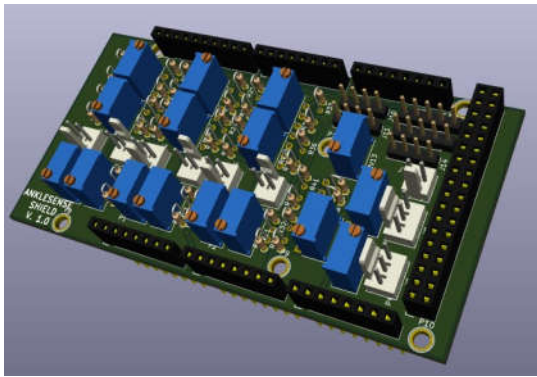


Fig. 6. Appearance of the circuit

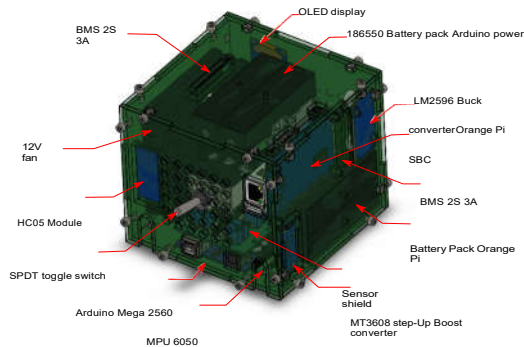


Fig. 7. Signal Conditioning circuit

attachment is sliced for section printing. A sensor arrays support is designed and made with laser cutting in MDF. Also, an foot attachment system is located in the platform, taking into account several sizes, by selecting sliding, bolt securing and laces for the foot. On the platform, the second MPU is located for mobile reference with respect to the base system.

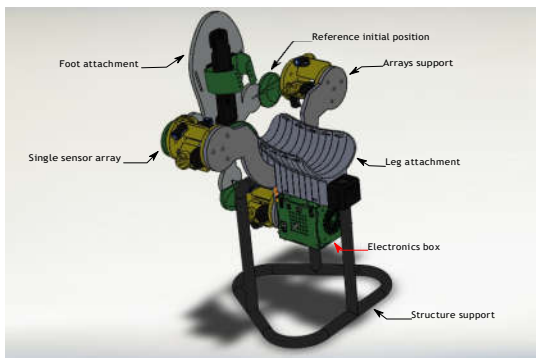


Fig. 8. Complete system

IV. FINAL DESIGN

The complete system appearance is showed in the figure. The system is designed for patients laying in bed or the floor.

V. CONCLUSIONS

The designed device can be used for fusion sensor and neural network training for kinematic model capture based in the



Fig. 9. Disposition of the device

correlation of the two sensors and the data from the draw wire systems. Once trained the systems, only with the MPU data the pose can be estimated. This device works with batteries and can be portable, the basic localization problem can be implemented in the Arduino. The SBC computer can be used for processing of the data and communication with Ethernet, visualization of the data in a screen and reprogramming the

Arduino.

ACKNOWLEDGMENT

The authors are grateful with the Universitat Politecnica de Valencia, Universidad de los Llanos, Colciencias and Colfuturo. These institutions were fundamental for the realization of this work.

REFERENCES

- [1] R. E. Isman, V. T. Inman, and P. M. Poor, "Anthropometric studies of the human foot and ankle," *Bull Prosthet Res*, vol. 11, no. 10, pp. 97–129, 1969. [Online]. Available: <http://www.rehab.research.va.gov/jour/69/6/1/97.pdf>
- [2] R. M. Murray, Z. Li, S. S. Sastry, and S. S. Sastry, *A Mathematical Introduction to Robotic Manipulation*. CRC Press, Mar. 1994, google-Books-ID: D_PqGKR07oIC.
- [3] A. Lundberg, O. K Svensson, G. Németh, and G. Selvik, *The axis of rotation of the ankle joint*, Feb. 1989, vol. 71.
- [4] A. K. Singh, K. D. Starkweather, A. M. Hollister, S. Jatana, and A. G. Lupichuk, "Kinematics of the Ankle: A Hinge Axis Model," *Foot & Ankle*, vol. 13, no. 8, pp. 439–446, Oct. 1992. [Online]. Available: <https://doi.org/10.1177/107110079201300802>
- [5] K. A. Kirby, "Subtalar Joint Axis Location and Rotational Equilibrium Theory of Foot Function," *Journal of the American Podiatric Medical Association*, vol. 91, no. 9, pp. 465–487, Oct. 2001. [Online]. Available: <http://www.japmaonline.org/doi/abs/10.7547/87507315-91-9-465>
- [6] D. Bruening and J. Richards, *Optimal ankle axis position for articulated boots.*, Aug. 2005, vol. 4.
- [7] S. Spooner and K. Kirby, *The subtalar joint axis locator: A preliminary report*, May 2006, vol. 96.
- [8] G. S. Lewis, K. A. Kirby, and S. J. Piazza, "Determination of subtalar joint axis location by restriction of talocrural joint motion," *Gait & Posture*, vol. 25, no. 1, pp. 63–69, Jan. 2007. [Online]. Available: <http://www.sciencedirect.com/science/article/pii/S096663620600004X>
- [9] G. S. Lewis, T. L. Cohen, A. R. Seisler, K. A. Kirby, F. T. Sheehan, and S. J. Piazza, "In vivo tests of an improved method for functional location of the subtalar joint axis," *Journal of Biomechanics*, vol. 42, no. 2, pp. 146–151, Jan. 2009. [Online]. Available: <http://www.sciencedirect.com/science/article/pii/S0021929008005216>
- [10] J. Leitch, J. Stebbins, and A. B. Zavatsky, "Subject-specific axes of the ankle joint complex," *Journal of Biomechanics*, vol. 43, no. 15, pp. 2923–2928, Nov. 2010. [Online]. Available: <http://www.sciencedirect.com/science/article/pii/S002192901000388X>

- [11] W. C. H. Parr, H. J. Chatterjee, and C. Soligo, "Calculating the axes of rotation for the subtalar and talocrural joints using 3D bone reconstructions." *Journal of biomechanics*, vol. 45, no. 6, pp. 1103–1107, Apr. 2012.
- [12] K. Van Alsenoy, J. De Schepper, D. Santos, E. Vereecke, and K. D'Août, *The Subtalar Joint Axis Palpation Technique: Part 1 – Validating a Clinical Mechanical Model.*, Jun. 2014, vol. 104.
- [13] J. A. Nichols, K. E. Roach, N. M. Fiorentino, and A. E. Anderson, "Predicting tibiotalar and subtalar joint angles from skin-marker data with dual-fluoroscopy as a reference standard," *Gait & Posture*, vol. 49, pp. 136–143, Sep. 2016. [Online]. Available: <http://www.sciencedirect.com/science/article/pii/S0966636216301102>
- [14] J. A I Prinold, C. mazzà, R. Di Marco, I. Hannah, C. Malattia, S. Magni-Manzoni, M. Petrarca, A. B Ronchetti, L. Tanturri de Horatio, P. van Dijkhuizen, S. Wesarg, and M. Viceconti, *A Patient-Specific Foot Model for the Estimate of Ankle Joint Forces in Patients with Juvenile Idiopathic Arthritis*, Sep. 2015, vol. 44.
- [15] S. S. Xie, "Kinematic and Computational Model of Human Ankle," in *Advanced Robotics for Medical Rehabilitation: Current State of the Art and Recent Advances*, ser. Springer Tracts in Advanced Robotics, S. S. Xie, Ed. Cham: Springer International Publishing, 2016, pp. 185–221. [Online]. Available: https://doi.org/10.1007/978-3-319-19896-5_7
- [16] R. A. Siston, A. C. Daub, N. J. Giori, S. B. Goodman, and S. L. Delp, "Evaluation of methods that locate the center of the ankle for computer-assisted total knee arthroplasty," *Clinical Orthopaedics and Related Research*, vol. 439, pp. 129–135, Oct. 2005.
- [17] O. Bottema and B. Roth, *Theoretical Kinematics*. Dover Publications, Jan. 2012, google-Books-ID: f8I4yGV9ocC.
- [18] L. W. Tsai and B. Roth, "Design of Dyads with helical, cylindrical, spherical, revolute and prismatic joints," *Mechanism and Machine Theory*, vol. 7, no. 1, pp. 85–102, Mar. 1972. [Online]. Available: <http://www.sciencedirect.com/science/article/pii/0094114X72900195>